IN-33
45767
p.15

NASA Technical Memorandum 105248
AIAA-91-3525

Neutron, Gamma Ray and Post-Irradiation Thermal Annealing Effects on Power Semiconductor Switches

G.E. Schwarze
Lewis Research Center
Cleveland, Ohio

and

A.J. Frasca
Wittenberg University
Springfield, Ohio

Prepared for the
Conference on Advanced Space Exploration Initiative Technologies
cosponsored by AIAA, NASA, and OAI
Cleveland, Ohio, September 4-6, 1991

NASA

NEUTRON, GAMMA RAY AND POST-IRRADIATION THERMAL ANNEALING EFFECTS ON POWER SEMICONDUCTOR SWITCHES

G. E. Schwarze
NASA Lewis Research Center
Cleveland, Ohio

A. J. Frasca
Wittenberg University
Springfield, Ohio

Abstract

The effects of neutrons and gamma rays on the electrical and switching characteristics of power semiconductor switches must be known and understood by the designer of the power conditioning, control, and transmission subsystem of space nuclear power systems. The SP-100 radiation requirements at 25 m from the nuclear source are a neutron fluence of 10^{13} n/cm^2 and a gamma dose of 0.5 Mrads. Experimental data showing the effects of neutrons and gamma rays on the performance characteristics of power-type NPN Bipolar Junction Transistors (BJTs), Metal-Oxide-Semiconductor Field Effect Transistors (MOSFETs), and Static Induction Transistors (SITs) are given in this paper. These three types of devices were tested at radiation levels which met or exceeded the SP-100 requirements. For the SP-100 radiation requirements, the BJTs were found to be most sensitive to neutrons, the MOSFETs were most sensitive to gamma rays, and the SITs were only slightly sensitive to neutrons. Post-irradiation thermal anneals at 300 K and up to 425 K were done on these devices and the effectiveness of these anneals are also discussed.

Introduction

High efficiency and low specific-mass power and control electronic components for future high capacity power space systems, such as those proposed for the NASA Space Exploration Initiative (SEI), will be required to function reliably for long time periods with operation most likely in harsh environments. For power systems using a nuclear energy source, this harsh environment will include a wide energy spectrum of neutrons and gamma rays emitted by the fission reaction. The neutron fluxes and gamma dose rates to which the electrical components will be subjected, will depend on both the type of shielding arrangement and the distance between the components and nuclear source. For example, for the SP-100 delivering 100 kW at 25 m from the nuclear source, the neutron flux is 4.5 x 10^4 n/cm^{2}s and the gamma dose rate is 8.15 rad/hr. These are relatively low rates, but for a projected 7 year mission, the neutron fluence is 10^{13} n/cm^2 and the gamma dose is 0.5 Mrads.

Both semiconductor power switches and control electronics will be required in the Power Conditioning and Control subsystem, and also in the Instrument and Control subsystem for the nuclear reactor. The performance characteristics of high power semiconductor switches and control electronics subjected to high levels of neutron fluences and gamma doses, and also possibly high temperatures, must be clearly known and understood by the designer of these subsystems if flawless mission operation is expected.

The NASA Lewis Research Center has an experimental test program underway to determine and assess the effects of nuclear radiation on the electrical and switching characteristics of commercial and developmental-type power semiconductor switches. The primary thrust of the experimental work is to clearly identify those switch characteristics most sensitive to either or both gamma rays and neutrons. The conduction of in-situ experimental tests enables the determination of the rates of degradation and failure mechanisms of the switch's characteristics as a function of gamma dose rate

and total dose, and neutron flux and fluence at a given temperature. The experimental results obtained under this program will permit the circuit designer to determine the useability of a particular type of semiconductor switch for a specified mission application.

The types of semiconductor switches to be experimentally tested under this program include power diodes, transistors, and thyristors. The transistors include the Bipolar Junction Transistor (BJT), the Metal-Oxide-Semiconductor Field Effect Transistor (MOSFET), the Insulated Gate Bipolar Transistor (IGBT), and the Static Induction Transistor (SIT). The thyristors include both the phase-control and inverter type Silicon Controlled Rectifier (SCR) and the MOS Controlled Thyristor (MCT). All the power devices investigated to date used silicon semiconductors. A new and emerging semiconductor technology being worked on today is silicon carbide (SiC). SiC switches offer the real possibility of higher temperature operation than silicon switches. As these SiC devices become available, their tolerance to radiation effects will be experimentally investigated.

This paper will give the experimental results showing the effects of neutrons, gamma rays, and post-irradiation thermal anneals on power-type NPN BJTs, N-channel enhancement mode MOSFETs, and N-channel SITs. A brief discussion of the effects of neutrons and gamma rays on electronic materials and devices will first be given.

Gamma Ray and Neutron Effects

The physics of radiation damage in semiconductor switches is quite complex and the effects of radiation on a switch's electrical and dynamic switching characteristics are dependent on the device's physics. The brevity of this paper does not allow a complete discussion of all of the effects associated with gamma rays, neutrons, and thermal annealing of radiation damage in electronic materials and devices, so the interested reader is referred to reference (1) and the references cited therein. A brief description of the interaction of gamma rays and neutrons with matter follows.

Gamma rays are high energy photons or quanta and can be produced when a nucleus decays from its excited state to another lower or ground state. Gamma rays interact with matter in three different ways: photoelectric effect, Compton scattering, and pair production. Electrons are emitted in each of these processes. In semiconductors and insulators, ionization produces electron-hole pairs; an electron is emitted and a mobile hole is generated in the valence band. About 3.6 eV is required to create an electron-hole pair in silicon. Charged particles such as electrons, protons, and alpha particles interact with atoms primarily by Rutherford scattering (Coulomb scattering). An ionized electron imparted with sufficient kinetic energy can cause additional ionization or displacement of atoms. In silicon the photoelectric effect dominates at photon energies less than 50 keV and pair production dominates at energies greater than 20 MeV with Compton scattering dominating in the intervening energy range. In semiconductor devices, the main effects of ionization are hole traps or positive charge build-up in the insulator (oxide) or passivation layer, electronic or interface states at the interface between the insulator and semiconductor, and photocurrents.

Neutron interactions with matter can be divided into two categories: capture and scattering. In the capture process the target nucleus absorbs the incident neutron to form a compound excited nucleus which subsequently decays to a stable nucleus through photon emission or charged particle emission (transmutation). In certain heavy nuclei the compound nucleus splits (fissions) into two separate fragments accompanied by the emission of neutrons and gamma rays. In scattering interactions the incident neutron remains free at a lower kinetic energy and part of the incident neutron's kinetic energy is transferred to the target nucleus known as the primary recoil or knock-on atom. In scattering interactions the target atom in crystalline materials can be displaced from its lattice site and for most materials about 25 eV is required to dislodge the atom. Displacement of atoms can cause either simple defects (vacancy-interstitial pairs) or complex local rearrangement of the atoms known as cluster defects. Through thermal motion some

of these displaced atoms become mobile and migrate through the lattice structure until they either recombine as vacancy-interstitial pairs, or form immobile stable defects, or escape to a free surface. In crystalline substances these atomic displacements alter the periodicity of the lattice. This disruption of lattice periodicity in a semiconductor or insulator leads to discrete energy levels in the material's bandgap. The presence of these discrete energy levels in the bandgap can cause several processes to occur: generation, recombination, trapping, removal, and tunneling of electron and hole carriers. Besides these processes, radiation induced atomic displacements generate carrier scattering centers which affect carrier mobility.

Experimental Setup

In the experimental test program the approach is to make all electrical and switching measurements of the power semiconductor switches under in-situ radiation and temperature conditions whenever possible. The approach consists of three main steps. The first step is to determine the effects of gamma dose rate and total dose, and neutron flux and fluence under room temperature conditions on the switch's characteristics. Post-irradiation thermal anneals for long periods of time at room temperature and short-term anneals at elevated temperatures are also part of this step. The next step is to determine the effects of gamma rays and neutrons at elevated temperatures. The possibility that the effects of neutrons and gamma rays on power semiconductor switches at temperatures well above room temperature will cause less permanent radiation damage needs to be fully investigated. Almost all of the devices irradiated to date were done at or near room temperature. The third and final step of the test program will be to integrate the semiconductor electronics and other electrical components in a circuit and determine degradation rates and failure mechanisms for the circuit when it is subjected to gamma and neutron irradiation and operating temperature conditions.

The research facilities and equipment of the NASA Lewis Research Center, Wittenberg University, Ohio State University (OSU), and the University of Cincinnati (UC) are used for the experimental tests, data analysis, and assessment of radiation damage. The OSU research reactor facility is used for neutron tests and the peak in the reactor's neutron energy spectrum is near 2 MeV. The UC Cobalt-60 facility is used for gamma ray tests and this facility consists of a large water pool with the Cobalt-60 source located about fifteen feet below the water surface. The use of a submerged Cobalt-60 source allows for a significant amount of gamma backscatter which reduces the gamma energy to which the devices are subjected. This broadened energy spectrum is typical of the energy for gamma rays emitted in a nuclear reactor due to fission fragment decay.

Almost all the devices irradiated to date were done at or near room temperature. Some initial neutron irradiation tests have been conducted recently at temperatures up to 365 K. The primary purpose of these tests was to test the adequacy of a newly fabricated high temperature fixture. The room temperature neutron and gamma irradiation tests lasted from several hours to days in order to obtain specific fluences or doses at controlled fluxes or dose rates, respectively. Several of the gamma irradiation tests were done at low dose rates to duplicate the gamma dose received by similar devices during reactor tests. It was found that the gamma dose received during the reactor tests for fluences on the order of 10^{13} n/cm^2 was only significant for power MOSFETs whose gate-source voltage is quite sensitive to ionization caused by gamma rays.

The test fixture for the gamma and neutron tests at room temperature is made from polyethylene and symmetrically holds up to four devices. The fixtures outer diameter is limited by the reactor's port hole diameter of six inches. The fixture's size does not cause any limitations in the experimental tests since the time required for the in-situ electrical measurements and analyses sets the upper bound on the number of devices which can be irradiated. Both power and sense cables are provided for each test device and these cables extend outside either the neutron or gamma ray source to the test instruments. The inner surface and the four individual test sockets of the fixture are lined with

cadmium to absorb the thermal neutrons, leaving only the epicadmium neutrons (0.5 eV to 10 MeV). Displacement of atoms in silicon requires about 25 eV so that the inclusion of thermal neutrons in the fluence is not a fair representation of the device's capability in terms of neutron hardness. Thermal neutrons primarily cause neutron activation, that is, transmutation, and minimization of neutron activation is highly desirable so that immediate post-irradiation tests can be conducted outside the reactor to monitor the effects of thermal annealing at room temperature.

A curve tracer is used to make the electrical measurements before, during, and after irradiation. These measurements consist of the ON-state current-voltage characteristic curves and the OFF-state leakage current-voltage breakdown curves. The data from these curves are used to plot the switch's electrical parameters as a function of either the neutron fluence or gamma dose. These plots clearly identify those electrical parameters most sensitive to either gamma rays or neutrons, or both, by graphical illustration of the degradation rates. Special drive circuits are designed for the switching-time tests for each of the different types of switches. Presently, the tests for determining switching times are conducted only before and after irradiation.

Upon completion of either a neutron or gamma irradiation test run, the electrical and switching characteristics are monitored to determine any post-irradiation changes in device characteristics at room temperature. Devices from each test run are also subjected to thermal anneals at elevated temperatures to determine any changes in device characteristics caused by radiation damage. The thermal anneal times at elevated temperatures are sufficiently long to ensure that any parameter changes have stabilized at the annealing temperature. Any changes in device characteristics appear to be complete in an hour at a specified temperature.

Experimental Results

Radiation and Annealing Effects in BJTs

The BJT is a current controlled device in which the base current I_B controls the output collector current I_C. The ratio of I_C to I_B is the DC current gain, h_{FE}. Physically, h_{FE} represents the fraction of majority carriers emitted by the emitter that pass through the base as minority carriers and collected as majority carriers by the collector.

Fast neutrons primarily cause cluster lattice defects and they are the dominant radiation induced damage mechanism in BJTs. Gamma rays are also capable of generating lattice defects by energetic electrons resulting primarily from Compton scattering. Lattice defects cause the formation of Recombination-Generation (R-G) centers. As the R-G center density increases with either increasing neutron fluence or gamma dose, the minority carrier recombination lifetime decreases so that the rate of electron-hole recombination increases in the base. Decreases in minority carrier lifetime causes decreases in both h_{FE} and the switching storage time. A decrease in switching storage time is beneficial because it reduces the switching losses. A decrease in h_{FE} is, of course, detrimental because I_C decreases for a constant I_B, or equivalently, I_B must increase to maintain a given I_C. A switching-type power BJT has a relatively low h_{FE} at rated I_C and forward collector-emitter voltage V_{CE}, so any degradation in h_{FE} impacts the switch's operational use. A decrease in h_{FE} does not make a switching-type power BJT inoperative as long as the device does not exceed its maximum continuous I_B rating, but a decrease in h_{FE} makes the BJT a more inefficient switch because the switch's total losses increase as I_B increases to maintain a given I_C.

The results given in Figures 1 through 12 are for a D60T455010 power NPN transistor and with manufacturer's ratings of h_{FE} = 10 at I_C = 50 A and V_{CE} = 2.5 V, maximum continuous I_B = 20 A, V_{CBO} = 500 V, and V_{CEO} = 450 V. Figures 1 through 9 show the effects of neutrons and post-irradiation thermal annealing on the characteristics of this transistor, while Figures 10 through 12 show the effects of gamma rays and post-irradiation thermal annealing.

Figure 1 is a plot of h_{FE} versus the epicadmium neutron fluence for three different I_C values. These curves clearly show the rate of degradation of h_{FE} with increasing fluence. The I_C = 10 A and 30 A curves are for a total fluence of 1.65×10^{13} n/cm^2. The I_C = 50 A curve

terminates at 0.74 x 10^{13} n/cm^2 because above this fluence, I_B exceeds 20 A. Extrapolation of the I_C = 50 A curve shows that as the fluence approaches 10^{13} n/cm^2, h_{FE} approaches unity.

Figure 2 is a different way of conveying the same type of information given in Figure 1. Specification sheets for BJT switches generally give plots of h_{FE} versus I_C to show the dependency of h_{FE} on I_C. Figure 2 gives four h_{FE} versus I_C curves; the top curve is for pre-irradiation conditions, while the next lower and two following curves are for increasing fluence levels. Like Figure 1, the results given in Figure 2 clearly show the decrease in h_{FE} with increasing fluence. It should be noted that the total background gamma dose of 37 krads shown in Figures 1 through 9 is due to fission fragment decay and this relatively low dose level had no significant effect on either the electrical or switching characteristics of this transistor as verified by independent gamma experiments.

Figure 3 shows the effects of post-neutron irradiation thermal annealing on h_{FE}. In this Figure the upper curve is the pre-irradiation h_{FE} versus I_C curve and the lower curve is the post-irradiation curve for a fluence of 1.65 x 10^{13} n/cm^2. The data points just above the lower curve are for post-irradiation thermal annealing conditions at 300 K for various periods of time, and at 425 K after 6 months at 300 K. The data for the 425 K thermal anneal was taken at 300 K. These results show that thermal anneals at 300 K for long periods of time cause no significant increase in h_{FE}. Likewise, no significant improvement in h_{FE} is caused by the 425 K thermal anneal. These annealing results indicate that the severe degradation in h_{FE} caused by neutrons at 300 K is permanent and can not be reversed for thermal annealing temperatures up to 425 K.

Figure 4 is a plot of forward V_{CE} versus I_B for various values of I_C. The lower set of three curves is for pre-irradiation conditions while the upper set of three curves is for a neutron fluence of 1.65 x 10^{13} n/cm^2. The lower (pre-irradiation) curves show that V_{CE} for a given I_C does not change for $I_B \geq 5$ A. The upper (post-irradiation) curves show that V_{CE} is affected by neutrons as follows: First, the post-irradiation set of curves are all displaced upward from the pre-irradiation set of curves so that this result shows that for a given I_C and I_B (i.e., a fixed h_{FE}), V_{CE} increases with fluence. Second, the post-irradiation curves show that V_{CE} increases as I_B decreases. A low V_{CE} is required for low conduction losses in the switch. Thus, the post-irradiation curves show that low conduction losses can only be obtained by using high I_B values; but high I_B means the base circuit must supply higher currents, and this results in higher losses in that circuit. High I_B values also cause increases in switching storage times, and this causes higher switching losses. Thus, even though the BJT is operable at this fluence level, its efficiency is degraded considerably.

Figure 5 is a plot of I_C versus the base-emitter voltage, V_{BE}, for various values of I_B. Comparison of the pre-irradiation (dashed lines) curves with the post-irradiation (solid lines) curves shows that neutrons have a negligible effect on the I_C versus V_{BE} curves. The post-irradiation curves terminate at lower values of I_C than the pre-irradiation curves because of the decrease in h_{FE} for this fluence level.

In a reverse-biased p-n junction the drift current dominates and this reverse current, usually referred to as the leakage current, consists of two components. The one component, the reverse saturation current, assumes a zero R-G rate in the depletion region of the junction while the other component assumes R-G does occur in the depletion region. Both current components increase as the minority carrier lifetime decreases (i.e., electron-hole generation rate increases) so that an increase in radiation induced defects causes an increase in leakage current. Thus, for a specified reverse biased collector-base voltage with open emitter, V_{CBO}, and specified collector-emitter voltage with open base, V_{CEO}, the respective leakage currents, I_{CBO}, and I_{CEO}, increase as the radiation induced defects increase, or equivalently, for specified I_{CBO} and I_{CEO}, V_{CBO} and V_{CEO}, respectively, decrease as the density of defects increases.

Figure 6 is a plot of V_{CEO} for I_{CEO} = 10 μA versus the epicadmium neutron fluence for four different D60T455010 devices. Two of the devices were tested at a flux of 7.55 x 10^8 n/cm^{2}s for a

fluence of 1.65 x 10^{13} n/cm^2 and the other two were tested for the same period of time but at half the flux to give half the fluence. The results show that the device with the lowest pre-irradiation V_{CEO} is the least affected by neutrons while the device with the highest pre-irradiation V_{CEO} is the most affected. The explanation of this would suggest at least two possibilities. The first is that the collector of the device with the low initial V_{CEO} is more heavily doped than the collector of the device with the high initial V_{CEO} and conclude that the higher the collector dopant level, the less susceptible the collector is to neutron induced lattice defects. The second possibility is that the device with low initial V_{CEO} has current paths external to the semiconductor, and conclude that these external leakage currents mask the semiconductor leakage currents for low fluences, but as the fluence increases and more lattice defects are generated, then the semiconductor leakage current begins to exceed the external leakage current. The acceptance of either or neither of these explanations would require the conduction of additional experiments. It should be noted that the V_{CBO} versus fluence curves for these same devices show similar results.

In Figure 7, for three of the same devices discussed in Figure 6, V_{CEO} is held constant at 400 VDC and I_{CEO} is plotted as a function of epicadmium neutron fluence. Figure 7 conveys similar information as that given in Figure 6. That is, the device with the highest pre-irradiation I_{CEO} shows only a small increase in I_{CEO} with increasing fluence, while the device with the lowest pre-irradiation I_{CEO} shows a very significant increase in I_{CEO} with increasing fluence.

Figure 8 gives a set of I_{CEO} versus V_{CEO} curves for one of the devices listed in Figures 6 and 7. The lower curve in Figure 8 is for pre-irradiation conditions, the upper is for a fluence of 1.65 x 10^{13} n/cm^2, and the curves in between show the effects of post-irradiation thermal annealing at 300 and 425 K. I_{CEO} clearly shows recovery 48 hours after neutron irradiation and considerable recovery after 6 months. A 425 K thermal anneal after the 6 months period at 300 K causes I_{CEO} to recover almost to its pre-irradiation value. It is possible that the I_{CEO} recovery shown for 6 months at 300 K occurred before that time since no I_{CEO} data was taken between 48 hours and 6 months. I_{CEO} shows excellent recovery compared to h_{FE} for similar annealing conditions. These I_{CEO} annealing results would indicate that the radiation damage in the collector is considerably less permanent than that in the base. At this time it is not obvious why the radiation damage in the collector responds to annealing treatment but this same treatment is not a cure for the radiation induced damage in the base.

The four states in the switching sequence of a BJT are OFF, turn-on, ON, and turn-off. The OFF-state, the non-conduction interval, is characterized by V_{CBO} and V_{CEO} and their respective leakage currents, I_{CBO} and I_{CEO}. The ON-state, the conduction interval, is characterized by h_{FE} at specified I_C and V_{CE} values. The turn-on time is the sum of the delay rise and rise time. During turn-on, excess minority carriers accumulate in the base as the BJT goes from cut-off through the active to the saturation region. Excess minority carrier charge accumulated during turn-on must all be removed during turn-off. The turn-off time is the sum of the storage and fall times. For a BJT operating in the saturation region, the storage time is the longest switching time compared to the other three intervals. The excess carrier charge accumulated during turn-on and the rate of recombination of this charge during turn-off is proportional to the minority carrier lifetime in the base.

Figure 9 shows the pre- and post-irradiation storage time for the two devices subjected to a fluence of 1.65 x 10^{13} n/cm^2 as a function of I_B for I_C = 40 A and collector supply voltage V_{CC} = 45 VDC. The post-irradiation curve clearly shows a significant reduction of over 100% in storage time due to the radiation induced defects. Post-irradiation thermal annealing procedures, similar to those shown in Figure 3 for h_{FE}, did not cause any significant changes in the post-irradiation switching times for these devices. The decrease in minority carrier lifetime caused by the neutron-induced atomic displacements clearly enhances the switching characteristics of BJTs but likewise, severely degrades the ON-state current gain and OFF-state forward blocking voltage capability.

The final three figures on BJTs show the

results of Co-60 gamma rays on the ON- and OFF-states of the same type of devices used for the neutron irradiations. Figure 10 is a plot of h_{FE} versus gamma dose for three different I_C values. These curves clearly indicate that high doses of gamma rays are capable of causing atomic displacements and generating lattice defects that cause h_{FE} to decrease with increasing dose.

In Figure 11, for the same device listed in Figure 10, the upper curve is the pre-irradiation h_{FE} versus I_C curve and the lower curve is the post-irradiation curve for a gamma dose rate of 92 krads/hr for a total gamma dose of 4.9 Mrads. The data points just above the lower curve are for post-irradiation thermal annealing conditions at 300 K for various periods of time, and at 425 K after 9.5 months at 300 K. The data for the 425 K thermal anneal was taken at 300 K. Just like the thermal annealing results for the neutron irradiated device, the annealing results for the gamma irradiated device show that both the long-term thermal anneals at 300 K and the 425 K thermal anneal have no significant effect on the recovery of h_{FE}. These experimental results would indicate that gamma irradiation at 300 K causes the formation of permanent damage sites which are unable to become mobile at a 425 K annealing temperature.

Figure 12 gives two I_{CEO} versus V_{CEO} curves for the same device listed in Figures 10 and 11. The bottom curve in Figure 12 is the pre-irradiation data and the top curve is the post-irradiation data. Gamma irradiation to 4.9 Mrads causes I_{CEO} to increase slightly and this change in I_{CEO} is almost completely reversed after a 9.5 month thermal anneal at 300 K. Analysis of the experimental data shows that some of the increase in I_{CEO} at 4.9 Mrads is caused by photocurrent, which is not caused by radiation induced damage. Thus, the response of I_{CEO} and h_{FE} to thermal annealing is the same for both neutron and gamma ray induced damage caused under 300 K conditions.

Radiation and Annealing Effects in MOSFETs

The MOSFET, which conducts current by majority carriers, is a voltage controlled device in which the gate-source voltage controls the output drain current. MOSFETs are of two types: depletion- and enhancement- mode. Both types can be either N- or P- channel devices. Depletion-mode MOSFETs turn on with zero gate-source voltage and are normally-on devices, so a gate voltage is required for turn-off and to maintain the drain-source blocking voltage in the OFF-state. Enhancement-mode MOSFETs are normally-off devices because a gate-source threshold voltage $V_{GS(th)}$ is required for turn-on. Turn-on is accomplished by developing a charge inversion layer in the semiconductor under the gate oxide to form the conducting channel. Both N- and P- channel enhancement-mode MOSFETs have been developed for power applications with N-channel devices having the largest selection of current and voltage ratings. Accordingly, N-channel enhancement-mode MOSFETs were the focus of our irradiation studies, and thus, these will be the basis for the discussion of radiation induced effects and the effects of post-irradiation thermal annealing. The devices investigated were a high voltage, low current device (MTM15N50); and a medium voltage, medium current device (IRF250). The manufacturer's specifications for the MTM15N50 are: drain-source breakdown voltage with gate-source shorted, BV_{DSS} = 500 V; continuous drain current, I_D = 15 A, $V_{GS(th)}$ = 4.5 V (max.), drain-source on-resistance, $R_{DS(ON)}$ = 0.4 ohms (max.) at I_D = 7.5 A and V_{GS} = 10 V. The manufacturer's specifications for the IRF250 are: BV_{DSS} = 200 V, I_D = 30 A, $V_{GS(th)}$ = 4 V (max.), and $R_{DS(ON)}$ = 0.085 ohms (max.) at I_D = 16 A and V_{GS} = 10 V.

Neutron irradiation of MOSFETs causes $R_{DS(ON)}$ to increase for fluences greater than 10^{13} n/cm^2. Radiation induced crystal defects caused by atomic displacements cause decreases in majority carrier density (carrier removal), and carrier mobility. The electrical conductivity is proportional to the product of majority carrier concentration and mobility so a reduction in channel and drift-region conductivity causes $R_{DS(ON)}$ to increase.

Figures 13 and 14 show the effects of neutrons on $R_{DS(ON)}$ for two MTM15N50s and two IRF250s, respectively. The four test devices were subjected to neutron fluxes from 3.78×10^7 n/cm^{2}s to 2.27×10^9 n/cm^{2}s for a total fluence of 3.8×10^{13} n/cm^2 and a background gamma dose of 85 krads. No bias voltages were applied

during irradiation except during brief time periods when the measurements were made. The MTM 15N50 (500 V/15 A) devices in Figure 13 begin to show a definite increase in $R_{DS(ON)}$ beyond 10^{13} n/cm^2 while the IRF 250 (200 V/30 A) devices in Figure 14 show only a very small increase in $R_{DS(ON)}$ beyond 10^{13} n/cm^2. These results indicate that the high voltage devices are more susceptible to neutrons than the medium voltage devices but in either case, both are immune to neutron fluences up to 10^{13} n/cm^2.

Gamma irradiation of MOSFETs primarily causes $V_{GS(th)}$ shifts through the ionization process. Ionizing radiation generates electron-hole pairs almost uniformly in the gate oxide. These electrons and holes are separated by an applied or radiation induced electric field in the oxide. The trapped holes in the oxide act like a positive gate-source voltage and cause charge inversion in the semiconductor near the oxide-semiconductor interface in the same way as an applied positive gate-source voltage. The positive charge build-up in an N-channel enhancement mode MOSFET causes a negative shift in $V_{GS(th)}$ so that a less positive bias is required for turn-on. Sufficient positive charge build-up can cause $V_{GS(th)}$ to be equal to or less than zero. For $V_{GS(th)} \leq 0$, the N-channel enhancement mode MOSFET behaves like an N-channel depletion-mode MOSFET and turns on when a drain-source voltage is applied. Once the enhancement-mode MOSFET has reached this state, a negative bias is required for turn-off and maintenance of the OFF-state. Gamma rays can also cause the formation of interface or surface states which can compensate the negative shift in $V_{GS(th)}$ caused by the positive charge build-up in the oxide. As the gamma dose increases, this compensation effect can increase to cause a decrease in the rate of negative shift in $V_{GS(th)}$ to the point that $V_{GS(th)}$ shifts positively.

The effects of Co-60 gamma rays on $V_{GS(th)}$ are shown in Figure 15 for two MTM15N50s and in Figure 16 for two IRF250s. The four devices were first subjected to a gamma dose rate of 33.8 krads/hr to give a dose of 67.6 krads, and then the dose rate was increased to 62.1 krads/hr until a total dose of 1.5 Mrads was reached. No bias voltages were applied during irradiation except during the test measurements. The $V_{GS(th)}$ versus dose curves in Figure 15 show that the two MTM 15N50s track each other quite well, and the same holds true for the two IRF250s in Figure 16. A comparison of the $V_{GS(th)}$ versus gamma dose curves in Figure 15 with those in Figure 16 shows that the response of $V_{GS(th)}$ to gamma rays is the same. The curves in Figures 15 and 16 clearly show that $V_{GS(th)}$ for both MOSFETs is very sensitive to gamma rays. These curves also show that at 1.5 Mrads, $V_{GS(th)}$ has become negative for the MTM15N50 and zero for the IRF250.

Figure 17 shows the effects of post-irradiation room and elevated temperature thermal annealing on $V_{GS(th)}$ normalized to its pre-irradiation value for the MTM15N50 and IRF250. The left portion of the plot gives a representation of the change in the normalized $V_{GS(th)}$ for a gamma dose up to 1.5 Mrads. The details of this portion of the graph were previously presented in Figures 15 and 16. The mid-section of Figure 17 represents the recovery in the normalized $V_{GS(th)}$ for each device after 30 days at 300 K. After this time period $V_{GS(th)}$ is now greater than zero for each device. However, the $V_{GS(th)}$ required for turn-on is considerably less than that required for pre-irradiation conditions. The right side of the plot in Figure 17 shows the change in the normalized $V_{GS(th)}$ as a function of annealing temperature up to 425 K. Each device was annealed at a starting temperature of 325 K and then in 20 K increments up to 425 K for time periods of 3 to 7 hours at each temperature. The devices were cooled to room temperature after each annealing temperature for the $V_{GS(th)}$ measurement. The thermal anneals at the elevated temperatures caused $V_{GS(th)}$ to increase slightly for the MTM15N50 but had no noticeable effect on the IRF250. Thus, it is concluded that the gamma induced positive charge build-up in the gate oxide is very stable because $V_{GS(th)}$ shows only a small improvement after the 30 day, 300 K thermal anneal, and no significant improvement for thermal anneals up to 425 K.

Radiation and Annealing Effects in SITs

The Static Induction Transistor (SIT) is a high voltage, power Junction Field Effect Transistor (JFET). The SIT is a voltage controlled device in which the gate-source voltage controls the output

drain current. The SIT is a normally-on switch that needs no gate-source voltage for turn-on but requires a gate voltage for both turn-off and maintenance of the blocking state. The SIT is a majority carrier device and can be thought of as a bar of n- or p- type semiconductor to form an N- or P- channel, respectively, in which the channel resistance, and hence the drain current, is controlled by varying the gate-source voltage. Because the SIT is a majority carrier device, and also because it has no gate oxide, the SIT is an extremely fast switch with switching times of tenths of microseconds for both turn-on and turn-off.

The current-voltage characteristics of a JFET are very dependent on the ratio of length to width of the drain-source current channel. The requirements for a switching-type power JFET are high drain current handling capability and low $R_{DS(ON)}$ for the ON-state and high forward blocking capability and low leakage current for the OFF-state. Neither the short- nor the long-channel JFET is acceptable as a power device. The power JFET, such as the SIT, is an intermediate vertical channel device that exhibits pentode-like characteristics at high drain currents and low gate reverse-bias voltages, and triode-like characteristics at low drain currents and high gate reverse-bias voltages. Even though high forward blocking voltages can be achieved for SITs, their ON-state voltage drop is quite high and thus, SITs have relatively low current carrying capability compared to power BJTs and MOSFETs with comparable blocking voltages. The ON-state voltage drop of the SIT can be reduced by operating it in the *bipolar* mode of operation, that is, by applying a positive gate bias to an N-channel device.

Because the SIT has no gate oxide it should be relatively insensitive to gamma rays compared to the MOSFET. The principle radiation damage mechanism in SITs is atomic displacements primarily caused by neutrons. The effect of atomic displacements in SITs is the same as in MOSFETs; $R_{DS(ON)}$ increases with fluence because channel conductivity decreases due to decreases in carrier mobility and majority carrier concentration.

The 2SK180 N-channel SIT was selected for neutron and gamma irradiation tests. The manufacturer's specifications for this device are gate-drain breakdown voltage = 600 V at I_D = 0.1 mA, gate-source breakdown voltage = 70 V at I_D = 0.1 mA, I_D (max.) = 20 A, I_D (continuous) = 8 A and $R_{DS(ON)}$ = 1.5 ohms at V_{GS} = 0 V and I_D = 2 A.

Figure 18 shows the effect of neutrons on $R_{DS(ON)}$ for the 2SK180. The test devices were subjected to neutron fluxes from 7.55×10^7 to 3.78×10^9 n/cm^{2}s for a total fluence of 5.1×10^{13} n/cm^2 and a background gamma dose of 94 krads. The top curve for $R_{DS(ON)}$ versus fluence in Figure 18 is for the SIT's normal mode of operation at V_{GS} = 0, while the bottom curve is for the *bipolar* mode of operation at I_{GS} = 10 A. A comparison of $R_{DS(ON)}$ prior to irradiation for V_{GS} = 0 V (normal mode) and I_{GS} = 10 A (*bipolar* mode) shows that $R_{DS(ON)}$ decreases almost five times when the SIT is operated in the *bipolar* mode. The curves in Figure 18 show that for both operating modes of the SIT, $R_{DS(ON)}$ first increases gradually as the fluence approaches 10^{13} n/cm^2 after which $R_{DS(ON)}$ begins a steeper climb. A 300 K thermal anneal for 70 days caused $R_{DS(ON)}$ to decrease about 10% from its post-irradiation value. A 425 K thermal anneal following the 300 K anneal had no significant effect on $R_{DS(ON)}$. Thus, the neutron induced damage in SITs irradiated at 300 K is quite stable since the damage sites remain immobile for annealing temperatures up to 425 K.

The 2SK180s were gamma irradiated at gamma dose rates of 10.15 to 55.1 krads/hr for a total dose of 1.8 Mrads. The only change detected in electrical characteristics was about a 30% increase in $R_{DS(ON)}$ at 1.8 Mrads when the device was operated in the *bipolar* mode at I_{GS} = 10 A. No change was observed in $R_{DS(ON)}$ when the SIT was operated in its normal mode at V_{GS} = 0 V.

Conclusions

This paper gives the experimental results for the effects of neutrons, gamma rays, and post-irradiation thermal anneals on the performance characteristics of power-type NPN BJTs, N-channel enhancement mode MOSFETs, and N-channel SITs. Each of these devices was exposed

to a minimum neutron fluence of 10^{13} n/cm^2 and gamma dose of 0.5 Mrads, which are the SP-100 requirements for the electronics at 25 m from the nuclear source. All of the devices were still operational after being tested to radiation levels which exceeded the minimum levels. Although the switches were still operational, one or more of the switch's parameters was definitely affected by either the neutrons or gamma rays.

The BJTs were found to be most sensitive to neutrons and least sensitive to gamma rays. A neutron fluence of 10^{13} n/cm^2 caused a very significant decrease in both h_{FE} and switching storage time, and a significant increase in I_{CEO} and I_{CBO}. These same BJT parameters were affected by gamma rays, but gamma doses greater than 0.5 Mrads were required to cause any significant changes. The N-channel enhancement mode MOSFETs were found to be most sensitive to gamma rays and least sensitive to neutrons. The MOSFET parameter most sensitive to gamma rays is $V_{GS(th)}$; $V_{GS(th)}$ approaches zero as the dose approaches 1 Mrad. $R_{DS(ON)}$ is the MOSFET parameter most sensitive to neutrons, but neutron fluences greater than 10^{13} n/cm^2 were required to cause significant increases in this parameter. The SITs were found to be neither sensitive to neutrons nor gamma rays for fluences to 10^{13} n/cm^2 and doses to 0.5 Mrads, respectively. For fluences beyond 10^{13} n/cm^2, $R_{DS(ON)}$ did begin to show a significant increase, but no significant increase was observed in $R_{DS(ON)}$ for gamma doses up to 1.8 Mrads.

Post-irradiation long-term thermal anneals at 300 K and short-term thermal anneals up to 425 K were conducted on samples of each of the irradiated devices to determine the extent of permanent radiation damage. For the BJTs, the thermal anneals had hardly any effect on h_{FE} and the storage time, but the anneals significantly affected I_{CEO} and I_{CBO}. The thermal anneals caused I_{CEO} and I_{CBO} to recover to almost their pre-irradiation values. For the MOSFETs the thermal anneals caused $V_{GS(th)}$ to recover somewhat from its post-irradiation value, but $V_{GS(th)}$ never came close to regaining its pre-irradiation value. For both the MOSFETs and SITs, the thermal anneals caused $R_{DS(ON)}$ to decrease only slightly below its post-irradiation value.

Acknowledgment

This research was sponsored by the NASA Lewis Research Center under the High Capacity Power element of the Civilian Space Technology Initiative.

Reference

1. Schwarze, G. E. and Frasca, A. J., "Neutron and Gamma Irradiation Effects on Power Semiconductor Switches" in Proc. of the 25th Intersociety Energy Conversion Engineering Conference, held in Reno, NV, August 12-17, 1990.

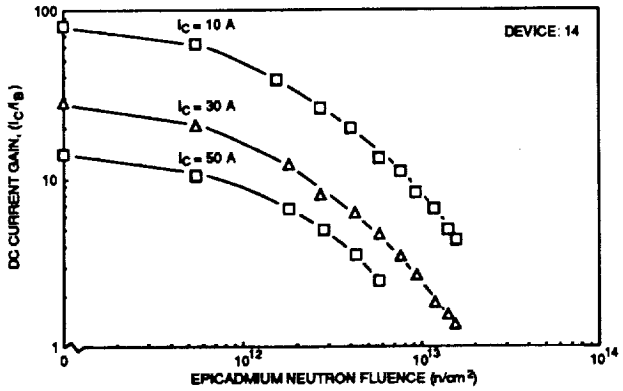

FIGURE 1. DC CURRENT GAIN @ V_{CE} = 2.5 V VERSUS FLUENCE FOR NPN TRANSISTOR D60T455010 (450 V/50 A). FLUX = 7.55×10^8 n/cm²s; GAMMA DOSE = 37 krad.

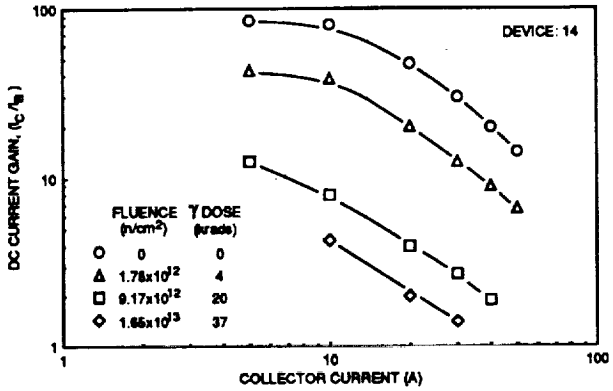

FIGURE 2. DC CURRENT GAIN @ V_{CE} = 2.5 V VERSUS COLLECTOR CURRENT FOR VARIOUS EPICADMIUM NEUTRON FLUENCES AND BACKGROUND GAMMA DOSES FOR NPN TRANSISTOR D60T455010 (450 V/50 A); NEUTRON FLUX = 7.55×10^8 n/cm²s.

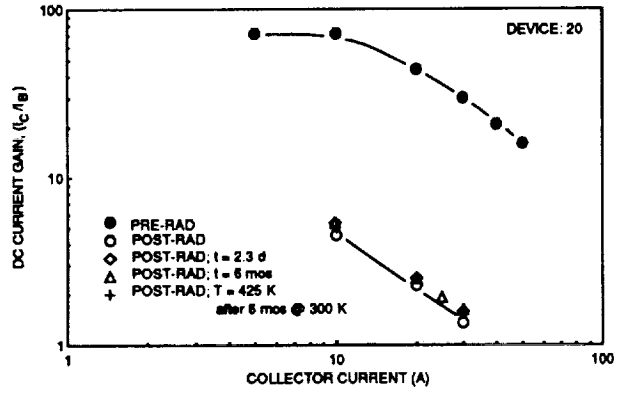

FIGURE 3. DC CURRENT GAIN @ V_{CE} = 2.5 V VERSUS COLLECTOR CURRENT FOR PRE-IRRADIATION, POST-IRRADIATION (FLUX = 7.55×10^8 n/cm²s, FLUENCE = 1.65×10^{13} n/cm², GAMMA DOSE = 37 krads), AND THERMAL ANNEALING CONDITIONS FOR NPN TRANSISTOR D60T455010. ALL MEASUREMENTS MADE AT 300 K.

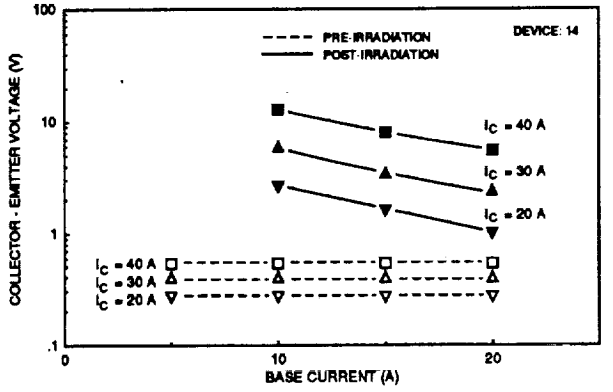

FIGURE 4. COLLECTOR - EMITTER VOLTAGE VERSUS BASE CURRENT FOR NPN TRANSISTOR D60T455010 (450 V/50 A); NEUTRON FLUX = 7.65×10^8 n/cm²s, FLUENCE = 1.65×10^{13} n/cm²; TOTAL GAMMA DOSE = 37 krads.

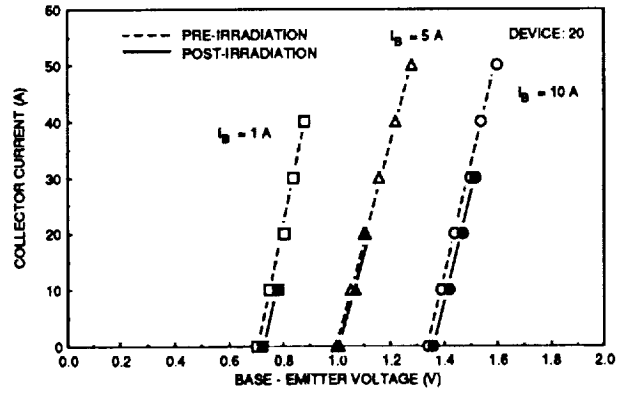

FIGURE 5. BASE-EMITTER VOLTAGE VERSUS COLLECTOR CURRENT FOR NPN TRANSISTOR D60T455010 (450 V/50 A); NEUTRON FLUX = 7.55×10^8 n/cm²s, FLUENCE = 1.65×10^{13} n/cm², TOTAL GAMMA DOSE = 37 krads

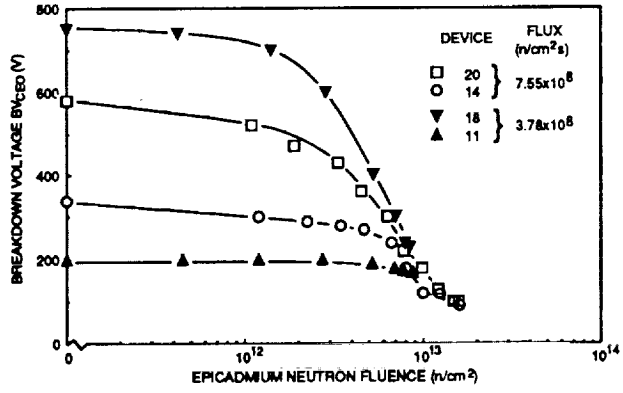

FIGURE 6. BREAKDOWN VOLTAGE BV_{CEO} @ I_{CEO} = 10 µA VERSUS FLUENCE FOR NPN TRANSISTOR D60T455010 (450 V/50 A), GAMMA DOSE: (20 & 14) = 37 krad; (18 & 11) = 18.5 krad.

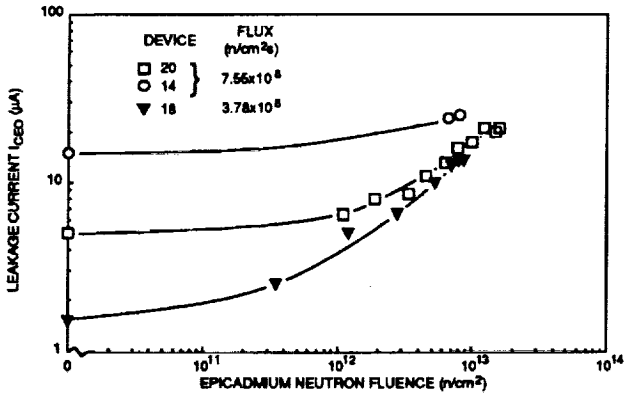

FIGURE 7. LEAKAGE CURRENT I_{CEO} @ V_{CEO} = 400 VDC VERSUS FLUENCE FOR NPN TRANSISTOR D60T45510 (450 V/50 A); TOTAL GAMMA DOSE (20 & 14) = 37 krads; (18) = 18.5 krads.

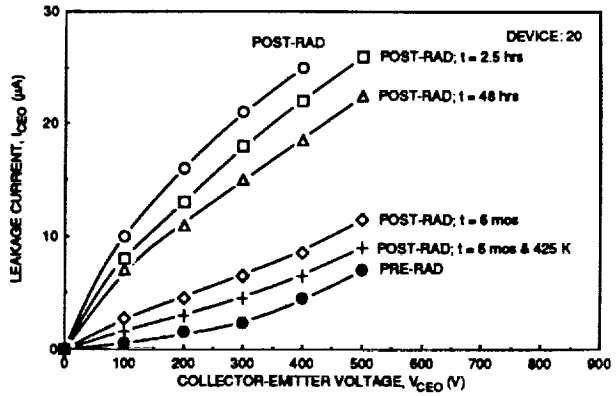

FIGURE 8. COLLECTOR-EMITTER LEAKAGE CURRENT VERSUS COLLECTOR-EMMITER VOLTAGE FOR NPN TRANSISTOR D60T455010 FOR PRE-IRRADIATION, POST-IRRADIATION (FLUENCE = 1.65×10^{13} n/cm^2 GAMMA DOSE = 37 krads), AND THERMAL ANNEALING CONDITIONS. ALL MEASUREMENTS MADE AT 300 K.

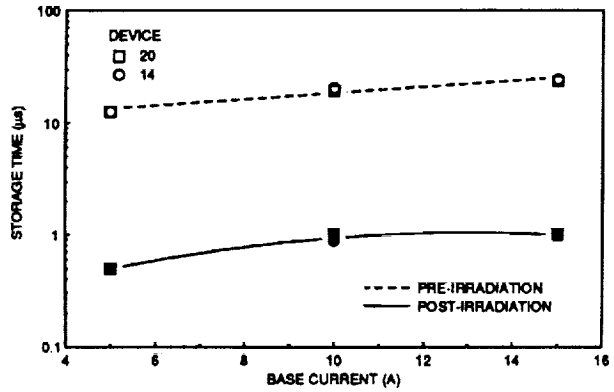

FIGURE 9. COLLECTOR CURRENT STORAGE TIME FOR I_C = 40 A AND V_{CC} = 45 V VERSUS BASE CURRENT FOR NPN TRANSISTOR D60T455010 (450 V/50 A); NEUTRON FLUX = 7.55×10^6 n/cm^{2}s, FLUENCE = 1.65×10^{13} n/cm^2, GAMMA DOSE = 37 krad.

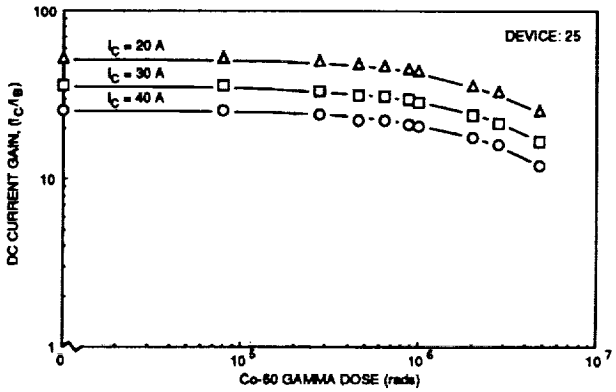

FIGURE 10. DC CURRENT GAIN @ V_{CE} = 2.5 V VERSUS Co-60 GAMMA DOSE FOR NPN TRANSISTOR D60T455010 (450 V/50 A); GAMMA DOSE RATE = 92 krads/hr.

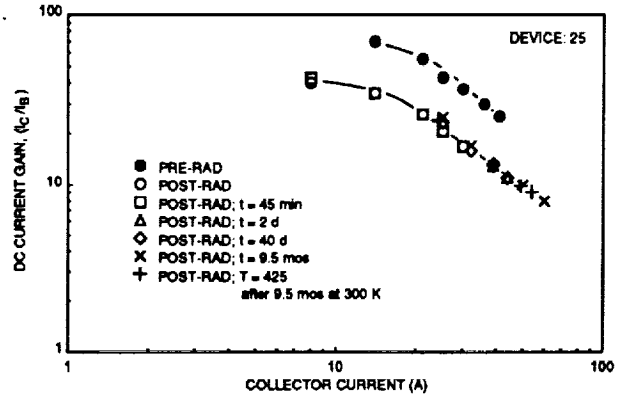

FIGURE 11. DC CURRENT GAIN @ V_{CE} = 2.5 V VERSUS COLLECTOR CURRENT FOR NPN TRANSISTOR D60T455010 (450 V/50 A) FOR PRE-IRRADIATION, POST-IRRADIATION (GAMMA DOSE = 4.9 Mrads) AND THERMAL ANNEALING CONDITIONS. ALL MEASUREMENTS MADE AT 300 K.

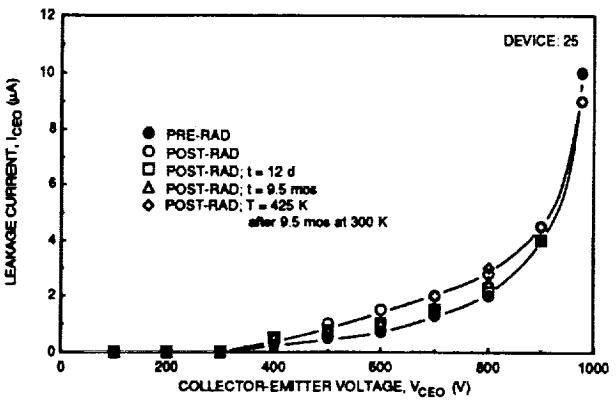

FIGURE 12. COLLECTOR-EMITTER LEAKAGE CURRENT VERSUS COLLECTOR-EMITTER VOLTAGE FOR NPN TRANSISTOR D60T455010 (450 V/50 A) FOR PRE-IRRADIATION, POST-IRRADIATION (GAMMA DOSE = 4.9 Mrads) AND THERMAL ANNEALING CONDITIONS. ALL MEASUREMENTS MADE AT 300 K.

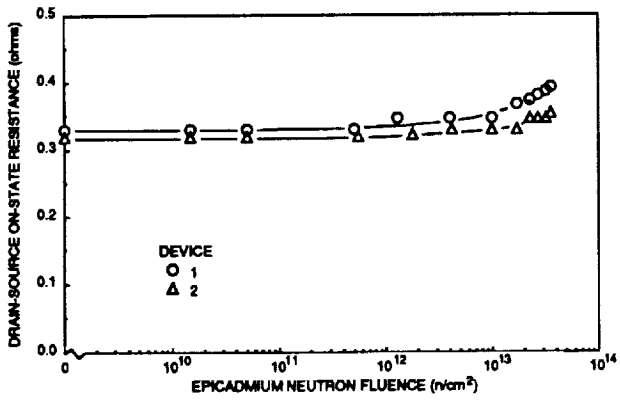

FIGURE 13. DRAIN-SOURCE ON-STATE RESISTANCE FOR I_D = 15 A AND V_{GS} = 10 V VERSUS EPICADMIUM NEUTRON FLUENCE FOR N-CHANNEL MTM15N50 (500 V/15 A); NEUTRON FLUX = 3.78×10^7 TO 2.27×10^9 n/cm²s, GAMMA DOSE = 85 krads.

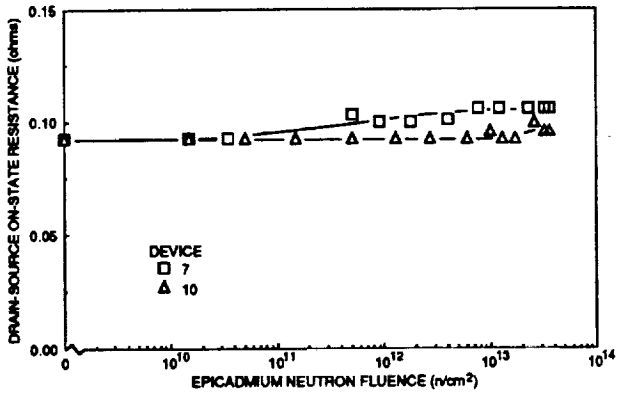

FIGURE 14. DRAIN-SOURCE ON-STATE RESISTANCE FOR I_D = 30 A AND V_{GS} = 10 V VERSUS EPICADMIUM NEUTRON FLUENCE FOR N-CHANNEL IRF250 (200 V/30 A); NEUTRON FLUX = 3.78×10^7 TO 2.27×10^9 n/cm²s, GAMMA DOSE = 85 krads.

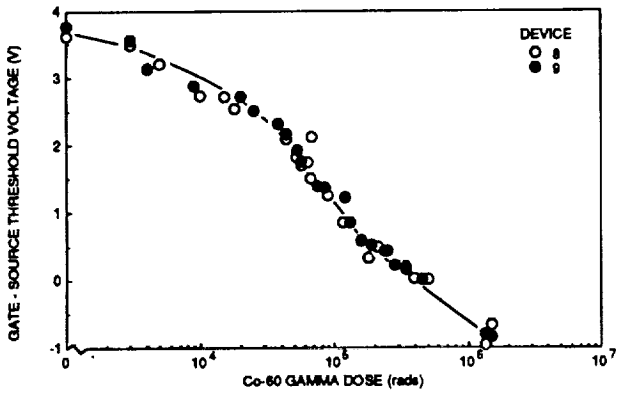

FIGURE 15. GATE-SOURCE THRESHOLD VOLTAGE VERSUS GAMMA DOSE FOR N-CHANNEL MTM15N50 (500 V/15 A); GAMMA DOSE RATE = 33.8 TO 62.1 krads/hr.

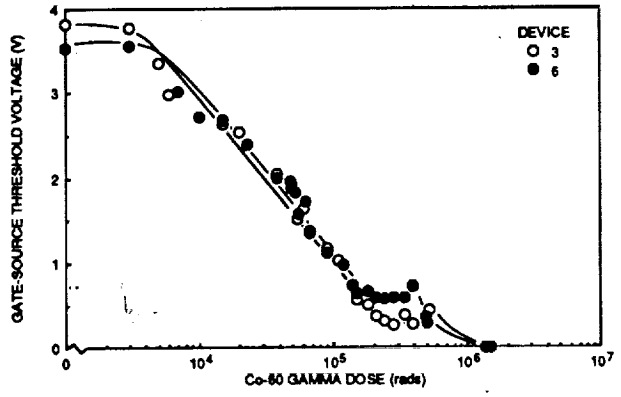

FIGURE 16. GATE-SOURCE THRESHOLD VOLTAGE VERSUS GAMMA DOSE FOR N-CHANNEL IRF250 (200 V/30 A); GAMMA DOSE RATE = 33.8 TO 62.1 krads/hr.

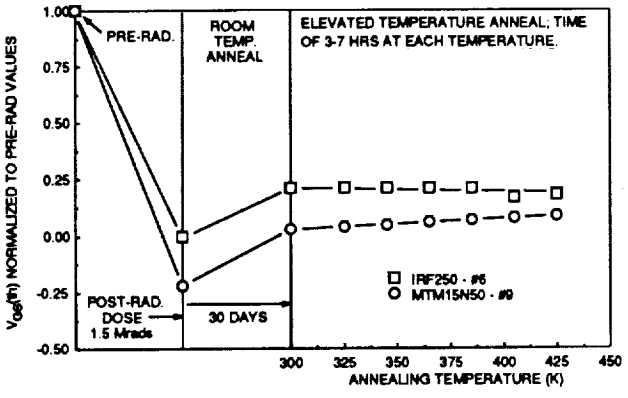

FIGURE 17. NORMALIZED GATE-SOURCE THRESHOLD VOLTAGE FOR N-CHANNEL MOSFETs MTM15N50 (500 V/15 A) AND IRF250 (200 V/30 A) FOR POST-IRRADIATION (GAMMA DOSE = 1.5 Mrads) AND THERMAL ANNEALING CONDITIONS. ALL MEASUREMENTS MADE AT 300 K.

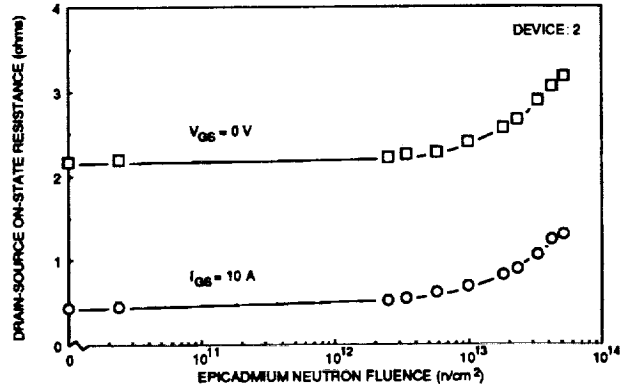

FIGURE 18. DRAIN-SOURCE ON-STATE RESISTANCE FOR I_D = 18 A VERSUS EPICADMIUM NEUTRON FLUENCE FOR N-CHANNEL 2SK180 (600 V/8 A); NEUTRON FLUX = 7.55×10^7 TO 3.78×10^9 n/cm²s, GAMMA DOSE = 94 krads.

REPORT DOCUMENTATION PAGE

Form Approved
OMB No. 0704-0188

1. AGENCY USE ONLY (*Leave blank*)	2. REPORT DATE	3. REPORT TYPE AND DATES COVERED
		Technical Memorandum

4. TITLE AND SUBTITLE

Neutron, Gamma Ray and Post-Irradiation Thermal Annealing Effects on Power Semiconductor Switches

5. FUNDING NUMBERS

WU-590-13-31

6. AUTHOR(S)

G.E. Schwarze and A.J. Frasca

7. PERFORMING ORGANIZATION NAME(S) AND ADDRESS(ES)

National Aeronautics and Space Administration
Lewis Research Center
Cleveland, Ohio 44135-3191

8. PERFORMING ORGANIZATION REPORT NUMBER

E-6577

9. SPONSORING/MONITORING AGENCY NAMES(S) AND ADDRESS(ES)

National Aeronautics and Space Administration
Washington, D.C. 20546-0001

10. SPONSORING/MONITORING AGENCY REPORT NUMBER

NASA TM-105248
AIAA-91-3525

11. SUPPLEMENTARY NOTES

Prepared for the Conference on Advanced Space Exploration Initiative Technologies cosponsored by AIAA, NASA, and OAI, Cleveland, Ohio, September 4-6, 1991. G.E. Schwarze, NASA Lewis Research Center; A.J. Frasca, Wittenberg University, Springfield, Ohio 45501. Responsible person, G.E. Schwarze, (216) 433-6117.

12a. DISTRIBUTION/AVAILABILITY STATEMENT

Unclassified-Unlimited
Subject Category 33

12b. DISTRIBUTION CODE

13. ABSTRACT (*Maximum 200 words*)

The effects of neutrons and gamma rays on the electrical and switching characteristics of power semiconductor switches must be known and understood by the designer of the power conditioning, control, and transmission subsystem of space nuclear power systems. The SP-100 radiation requirements at 25 m from the nuclear source are a neutron fluence of 10^{13} n/cm^2 and a gamma dose of 0.5 Mrads. Experimental data showing the effects of neutrons and gamma rays on the performance characteristics of power-type NPN Bipolar Junction transistors (BJTs), Metal-Oxide-Semiconductor Field Effect Transistors (MOSFETs), and Static Induction Transistors (SITs) are given in this paper. These three types of devices were tested at radiation levels which met or exceeded the SP-100 requirements. For the SP-100 radiation requirements, the BJTs were found to be most sensitive to neutrons, the MOSFETs were most sensitive to gamma rays, and the SITs were only slightly sensitive to neutrons. Post-irradiation thermal anneals at 300 K and up to 425 K were done on these devices and the effectiveness of these anneals are also discussed.

14. SUBJECT TERMS

Radiation damage; Radiation effects; Power transistor; Solid state switch; Semiconductor switch; MOSFET; SIT; Power conditioning

15. NUMBER OF PAGES

14

16. PRICE CODE

A03

17. SECURITY CLASSIFICATION OF REPORT	18. SECURITY CLASSIFICATION OF THIS PAGE	19. SECURITY CLASSIFICATION OF ABSTRACT	20. LIMITATION OF ABSTRACT
Unclassified	Unclassified	Unclassified	